On the role of subunit M in cytochrome cbb3 oxidase

Carvalheda , Catarina A.; Pisliakov, Andrei V.

Published in:
Biochemical and Biophysical Research Communications

DOI:
10.1016/j.bbrc.2017.07.031

Publication date:
2017

Accepted Manuscript

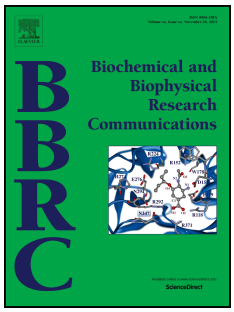

On the role of subunit M in cytochrome *cbb*$_3$ oxidase

Catarina A. Carvalheda, Andrei V. Pisliakov

PII: S0006-291X(17)31373-6

DOI: 10.1016/j.bbrc.2017.07.031

Reference: YBBRC 38137

To appear in: *Biochemical and Biophysical Research Communications*

Received Date: 4 July 2017

Revised Date: 0006-291X June 0006-291X

Accepted Date: 6 July 2017

Please cite this article as: C.A. Carvalheda, A.V. Pisliakov, On the role of subunit M in cytochrome *cbb*$_3$ oxidase, *Biochemical and Biophysical Research Communications* (2017), doi: 10.1016/j.bbrc.2017.07.031.

On the role of subunit M in cytochrome *cbb*$_3$ oxidase

Catarina A. Carvalheda[ab*], Andrei V. Pisliakov[ab*]

[a]Computational Biology, School of Life Sciences, University of Dundee, Dow Street, Dundee, DD1 5EH, United Kingdom

[b]Physics, School of Sciences and Engineering, University of Dundee, Nethergate, Dundee, DD1 4HN, United Kingdom

*Corresponding authors:

E-mail addresses: c.a.c.dossantos@dundee.ac.uk, a.pisliakov@dundee.ac.uk

Abstract

Cytochrome *cbb*$_3$ (or C-type) oxidases are a highly divergent group and the least studied members of the heme-copper oxidases (HCOs) superfamily. HCOs couple the reduction of oxygen at the end of the respiratory chain to the active proton translocation across the membrane, contributing to establishment of an electrochemical gradient essential for ATP synthesis. *Cbb*$_3$ oxidases exhibit unique structural and functional features and have an essential role in the metabolism of many clinically relevant human pathogens. Such characteristics make them a promising therapeutic target. Three subunits, N, O and P, comprise the core *cbb*$_3$ complex, with N, the catalytic subunit, being highly conserved among

all members of the HCO superfamily, including the A-type (aa_3, mitochondrial-like) oxidases. An additional fourth subunit containing of a single transmembrane (TM) helix was present in the first crystal structure of cbb_3. This TM segment was recently proposed to be part of a novel protein CcoM, which was shown to have a putative role in the complex stability and assembly. In this work, we performed large-scale all-atom molecular dynamics simulations of the CcoNOPM complex to further characterize the interactions between subunit M and the core subunits and to determine whether the presence of the 4th subunit influences the water/proton channels previously described for the core complex. The previously proposed putative CcoNOPH complex is also assessed, and the potential functional redundancy of CcoM and CcoQ is discussed.

Keywords: molecular dynamics, proton transfer, water dynamics, cytochrome c oxidase, proton pump, membrane protein

1. Introduction

Heme-copper oxidases (HCOs) are membrane bound enzymatic complexes that terminate the respiratory chains of aerobic organisms. They catalyse the oxygen reduction to water and couple the energy released during this reaction to the active proton translocation from the negative to the positive side of the membrane, thereby contributing to the establishment of a proton motive force, which drives ATP synthesis [1,2]. Here we focus on distinctive cbb_3 (or C-type) oxidases, which are mostly present in bacteria and represent the second most abundant group in the HCO superfamily. These enzymes exhibit several unique features and are essential for survival of many pathogenic bacteria (e.g. *Campylobacter jejuni*, *Neisseria*

gonorrhoeae, *Helicobacter pylori*), which makes them a promising pharmacological target [3–6]. The cbb_3 complex comprises three core subunits (Figure 1): the catalytic subunit N (CcoN or I), which has the same architecture as the central subunit in A- and B-type HCOs, and subunits O (CcoO or II) and P (CcoP or III), which share no similarity with subunits found in A- or B-type families [3]. Assembly of the cbb_3 complex has been mainly studied in *Rhodobacter capsulatus* [7–10], and shown to involve the formation of two intermediate subcomplexes: CcoNO and CcoQP, each stabilized by a copy of the assembly factor. In the subsequent steps, subunit P is attached to the CcoNO subcomplex yielding a fully active cbb_3 complex.

The structure of cbb_3 from *P. stutzeri* (isoform 1, Cbb3-1) was determined at a resolution of 3.2 Å [3]. In addition to three core subunits (N, O, and P), the electron density map revealed presence of a fourth subunit consisting of a single TM helix located near helices VIII, IX, and XI of subunit N. This TM segment could not be assigned to subunit Q, the known accessory subunit in cbb_3 oxidases [3]. Hence, its nature and role remained unclear.

In a recent study [11], this TM segment was assigned to an assembly factor H and reconstituted as the fourth subunit into the *P. stutzeri* X-ray structure. Following this assignment, the authors built a model of the CcoNOPH complex and using computational methods predicted a water channel lining a large solvent-accessible but mostly hydrophobic cavity formed at the interface of subunits N and H. Such channel was observed to connect the cytoplasm in the vicinity of the residue R308 with the residue E323, which is H-bonded to the proximal ligand of heme b_3 (H345) and had been suggested to be part of the so-called proton loading site (PLS) in cbb_3 [12,13]. Furthermore, as this new water channel bypasses the K_C-channel and the active site, the authors suggested it to work as an additional proton pumping pathway in *P. stutzeri* cbb_3, thus having an important role in the pumping mechanism and in the cbb_3 overall function [11].

The assignment of the fourth subunit to subunit H was recently challenged by Michel and co-workers [14], who proposed the TM helix to be part of a novel protein CcoM (or subunit M). CcoM was shown to have a putative role in the cbb_3 complex assembly and stability, while its absence was shown to have no impact on the enzymatic activity of cbb_3 [14]. The successful reconstitution of subunit M into the electron density of the fourth subunit in *P. stutzeri* X-ray structure – and thus, the CcoNOPM complex – showed [14] ladder-like interactions between subunit M and helices VIII and IX of the catalytic subunit N (Figure 1C). Subunit M is almost exclusively present in species of the genus *Pseudomonas* [14] and has structural resemblance and shares conserved residues with subunit Q (Figure 2D). Subunit Q was also shown to be involved in the complex assembly but not required for the enzymatic activity [10,15]. Based on these observations, subunits M and Q were suggested to be functionally redundant, but definite conclusions require further studies [14,15].

Recently, we have provided insights into proton translocation pathways of cbb_3 oxidase, which was modelled as the core CcoNOP complex [12]. Here we extend the simulation study by including the fourth subunit M – and thus, the CcoNOPM complex – with the objective of further characterizing the interactions between the core subunits and the TM segment of subunit M and examining whether the presence of the fourth subunit has an impact on the previously described water/proton channels. Our results suggest that subunit M maintains persistent interactions with subunit N without affecting the previously observed internal water channels or leading to the formation of new ones. This is in line with the experimental observations which showed that the presence of CcoM does not affect the catalytic or pumping activities of Cbb3-1 from *P. stutzeri* [14].

2. Materials and Methods

The crystal structure of the *P. stutzeri cbb*$_3$ complex containing three core subunits (N, O, P) and an additional TM helix, reconstituted as part of subunit M, (chains A, B, C and N from PDB ID: 5DJQ) [3,14] was used as the initial protein configuration. The system setup followed the protocol described elsewhere for the CcoNOP complex [12]. The final system contained 414 lipid molecules and a total of ~208K atoms. MD simulations were performed according to the protocol described in our previous work [12], using GROMACS version 5.0.2 [16,17], with CHARMM36 force field [18–20] and in-house parameterisation of the reduced redox centres. Three replicas (R1, R2 and R3) were generated using different initial velocities and simulated for 350 ns each. Based on previous pK_a calculations [12], all ionisable residues were modelled in the default protonation states. All histidine residues were taken neutral, except for H243^N, H337^N and H124^O, which where simulated in the charged (protonated) state. [Throughout the paper, the superscripts above the residue number denote the subunit – N, O, P, or M.] Due to the absence of the cytoplasmic part of subunit M, which would contain charged residues that help anchoring to the membrane (Figure 2D), the terminal residue of the TM segment, namely W29^M, was not capped, i.e. was modelled with the negatively charged C-terminal group. In all simulations, the TM region of the core complex remains very stable (rmsd values around 1 Å).

3. Results

3.1. Interactions of subunit M with core subunits

The C-terminal part of the TM segment of subunit M was previously shown [14] to tightly interact with helices XIII and IX of subunit N in a “ladder-like” fashion, involving the

following pairs of residues: $M17^{M}$-$F322^{N}$, $F20^{M}$-$W284^{N}$, $F20^{M}$-$M287^{N}$, $F20^{M}$-$F322^{N}$, $F24^{M}$-$M287^{N}$, and $F24^{M}$-$M291^{N}$ (Figure 1C). Residues $M17^{M}$ and $F20^{M}$ were shown to be highly conserved in all subunit M homologues, while $F24^{M}$ is sometimes replaced by valine or leucine (Figure 2D). We started by analysing the structural stability of subunit M by means of its root-mean-square deviation (rmsd) and fluctuation (rmsf) values, along with the persistency of the "ladder-like" interactions at the interface with subunit N (Figure 2 and Table 1). Our results showed that the TM segment of subunit M is very stable in all simulations, with slightly higher deviations in replica R3 (Figure 2). The most flexible part in all replicas was the N-terminal region of subunit M (residues 1 to 5) (Figure 2B), due to its disordered nature and some degree of solvent exposure. The higher rmsd values in R3 are attributed to the C-terminal region (Figure 2A and 2B), and these are likely due to the absence of the cytoplasmic part of subunit M, which would anchor it to the membrane. We observed that subunit M remains tightly attached to the core complex in the simulations (Figure 2C), and that most of the "ladder-like" interactions remain stable (Table 1). There are slight variations for contacts involving $F20^{M}$ and $F24^{M}$ at the C-terminal region of the TM helix due to the unanchored C-terminus. For example, $F24^{M}$-$M291^{N}$ is less tight in R2, while $F20^{M}$-$W284^{N}$ distances greater in both R1 and R3, and $F20^{M}$-$F322^{N}$, $F24^{M}$-$M287^{N}$, $F24^{M}$-$M291^{N}$ are disrupted in R3. The loss of such interactions in R3 is probably related with the higher degree of flexibility measured for the TM region of subunit M in this replica (Figure 2B). The $F20^{M}$-$M287^{N}$ distance increases to ~7 Å in all replicas revealing a labile nature mainly due to the flexibility of the $F20^{M}$ phenyl ring. In addition to the contacts reported by Michel and co-workers [14], we found that the "ladder-like" interactions extended to the N-terminal part of subunit M and involved the following pairs of residues: $V6^{M}$-$T331^{N}$, $G10^{M}$-$L335^{N}$, $G10^{M}$-$V332^{N}$, $T13^{M}$-$V332^{N}$, $T13^{M}$-$M326^{N}$, $L16^{M}$-$M326^{N}$ (Figure 1B and Table 1). Residues $G10^{M}$ and $T13^{M}$ where shown to be conserved in subunit M homologues (Figure

2D), while $L16^M$ is sometimes replaced by a valine [14]. These interactions show great stability in our simulations and agree well with the crystal structure.

There are no significant interactions between subunit M and subunits O or P.

3.2. Internal hydration of cbb_3 in the presence of subunit M

Identifying proton transfer pathways and understanding the coupling mechanism between proton pumping and catalytic reaction at BNC is the long-standing goal of studies that focus on cytochrome *c* oxidases. Accurate description of the internal water distribution is therefore an important issue to address. In this section we investigate whether the presence of subunit M: i) affects the formation of a previously observed water connectivity in the K_C-channel [12,13], and ii) leads to the formation of new channel(s) at the interface with the core complex, as it was suggested for subunit H [11]. In agreement with our previous results for the core complex [12], a stable continuous water channel in the K_C-channel, connecting the cytoplasmic side of the membrane with the active site, is also observed in the presence of subunit M (simulations R1-3, with H243 positively charged). The water distribution in the K_C-channel was further analysed by sub-dividing the channel into three regions: top, bottom and bottleneck (Figure 3A). Compared to our previous study, we observed similar levels of hydration in each of the regions: top (~ 6), bottleneck (~6) and bottom (~12). The bottleneck region is well hydrated and the number of waters populating this region is modulated by interactions and sidechain dynamics of residues H243, Y233, N289 and S240 (data not shown) as discussed before [12]. A substantial increase in the number of waters in the bottom region is observed in R1 at ~290 ns. This is due to the formation of an additional stable water intake pathway (see below).

The bifurcation region was previously proposed to be part of the proton exit pathway [12,13]. The formation of a continuous water channel in this region, bridging Y317 and E323, was

observed in our previous simulations of the core complex, but only when H337, a likely PLS, was modelled in the neutral state. In the present work H337 is kept in the charged state. In line with the previous results [12], no waters were observed in the bifurcation region during the present simulations for the CcoNOPM complex (Figure 3A and Figure 3B). Interestingly, the results for the water occupancy (Figure 3B) and number of waters (Figure 3C) reveal an increased local hydration of E323 (~2-3 extra water molecules) in simulation R3. This is a result of the disruption of the $G10^{M}$-$V332^{N}$ and $L16^{M}$-$M326^{N}$ interactions at the interface between subunits M and N (Figure 2B and Table 1).

The water/proton intake pathways from the bulk into the K_C-channel observed in the presence of subunit M are also in agreement with our previous results for the core complex [12], namely the $E48^{P} \rightarrow E49^{P}$ and $E8^{O} \rightarrow Y237^{N} \rightarrow E49^{P}$ pathways (Figure 4A). In addition, the previously observed alternative route $N52^{P} \rightarrow Y235^{N} \rightarrow N298^{N} \rightarrow H243^{N}$ is also transiently observed in R3 (Figure 4A). In simulation R1, the sidechain of the residue $Y235^{N}$ flips downwards and, together with $R232^{N}$, favours the formation of an extra pathway directly towards the bottleneck region, which is stabilised at around 290 ns (Figure 4B). This results in an increase in the number of waters populating the bottom region of the K_C-channel observed at around 290 ns in R1 (Figure 3A), as discussed in the previous section (3.1). These results confirm substantial versatility of the water/proton uptake routes from the bulk. Notably, all these pathways involve highly conserved residues and are consistent with the mutagenesis data [21–23].

A closer look at the interface between subunits M and N reveals that the presence of subunit M does not lead to formation of additional water channels (Figure 3B), which could be involved in the translocation of chemical and/or pumped protons. No waters are observed at the interface, which is not surprising given the presence of multiple “ladder-like” hydrophobic contacts that block the water access. Furthermore, the estimated pK_a values of

the residues H337 and E323 (modelled here in the charged state) do not significantly change due to the presence of subunit M: 11.5 *vs* 12.3 for H337 and 4.5 *vs* 5.7 for E323 in the presence (this work) and absence [12] of subunit M, respectively.

4. Discussion

In this work, we have carried out all-atom molecular dynamics simulations of the CcoNOPM complex from *P. stutzeri* with a twofold aim: i) to analyse the mode of association between the core subunits and recently identified fourth subunit, M, and ii) to understand whether the presence of CcoM affects formation of the proton translocation pathways previously identified for the CcoNOP complex [12]. All the "ladder-like" interactions between helices VIII and IX of the catalytic subunit CcoN and the C-terminal part of the TM helix of CcoM [14] were confirmed in our simulations, except for $F20^{M}$-$M287^{N}$, which exhibits a labile nature due to the conformational flexibility of the sidechain of $F20^{M}$. Furthermore, we have observed that this "ladder-like" pattern extends to the N-terminal part of the CcoM TM helix. Despite the extent of this contact interface, the presence of CcoM does not interfere with the stability of the CcoNOP complex throughout simulations (rmsd values of the TM region: ~1.02 Å with and ~1.20 Å without CcoM). Nevertheless, it most likely explains the reduced thermal stability observed experimentally in the absence of CcoM [14]. Our results are in line with the experimental evidence that CcoM does not interfere with the catalytic activity of cbb_3 [14].

We observed that the presence of CcoM does not affect internal water channels observed in previous works [12,13,21] or lead to the formation of additional ones. The same uptake pathways from the cytoplasm were observed as in our previous work [12], involving residue $E49^{P}$, an entry point to the K_C-channel [21,23]. These results agree with the experiments in

which CcoM was shown not to affect the enzymatic or proton pumping activities [14]. Interestingly, we have observed two alternative water intake pathways: the transient $N52^{P}$ → $Y235^{N}$ → $N298^{N}$ → $H243^{N}$ water connection, also observed in the CcoNOP complex [12], and a route via $Y235^{N}$ and $R232^{N}$ directly to the bottleneck region. These alternative routes could be responsible for some residual activity in $E49^{P}$/A variants [21,23].

To test the hypothesis put forward by Skulachev and co-workers [11] we also performed simulations for the putative CcoNOPH complex (Figure S1A). In contrast to that proposal [11], we conclude that CcoNOPH does not harbour an extra proton pumping channel as we have not observed the formation of a water connectivity between the cytoplasm and E323 at the interface between CcoH and the core complex (Figure S2A). Together with the recent unambiguous assignment of the fourth subunit to CcoM, our observations suggest that consequences of the presence of CcoH for the *P. stutzeri* cbb_3 pumping/functioning mechanism can be ruled out.

In summary, the presence of the fourth subunit (M or H) does not affect the proton transfer pathways or stability of the core complex in *P. stutzeri*. Due to the structural resemblance and conservation of the residues involved in the "ladder-like" interactions, subunits CcoM and CcoQ were initially hypothesised to be located at a similar position and have a redundant function in *P. stutzeri* [14]. However, CcoM and CcoQ only share a low degree of sequence identity (<20%) [15], and the contrasting results obtained for the strains lacking either CcoM or CcoQ [14,15] hint at different functional roles and locations of these two subunits in the cbb_3 complex. Therefore, our observations for the Cbb3-1 CcoNOPM complex might be extended to Cbb3-2, under the assumption that CcoM has same location in both isoforms, but should not hold for a putative CcoNOPQ complex.

Acknowledgments

This work was funded by the Scottish Universities Physics Alliance (SUPA). Access to ARCHER National Supercomputing Service was provided through the HEC-Biosim Consortium. We also appreciate support from the University of Dundee Life Sciences Computing cluster.

References

[1] M. Wikström, V. Sharma, V.R.I. Kaila, J.P. Hosler, G. Hummer, New Perspectives on Proton Pumping in Cellular Respiration, Chem. Rev. 115 (2015) 2196–2221. doi:10.1021/cr500448t.

[2] S. Yoshikawa, A. Shimada, Reaction Mechanism of Cytochrome c Oxidase, Chem. Rev. 115 (2015) 1936–1989. doi:10.1021/cr500266a.

[3] S. Buschmann, E. Warkentin, H. Xie, J.D. Langer, U. Ermler, H. Michel, The structure of cbb3 cytochrome oxidase provides insights into proton pumping, Science. 329 (2010) 327–330. doi:10.1126/science.1187303.

[4] Y. Huang, J. Reimann, L.M.R. Singh, P. Ädelroth, Substrate binding and the catalytic reactions in cbb3-type oxidases: The lipid membrane modulates ligand binding, Biochim. Biophys. Acta BBA - Bioenerg. 1797 (2010) 724–731. doi:10.1016/j.bbabio.2010.03.016.

[5] F. Melin, H. Xie, T. Meyer, Y.O. Ahn, R.B. Gennis, H. Michel, P. Hellwig, The unusual redox properties of C-type oxidases, Biochim. Biophys. Acta BBA - Bioenerg. 1857 (2016) 1892–1899. doi:10.1016/j.bbabio.2016.09.009.

[6] R.S. Pitcher, N.J. Watmough, The bacterial cytochrome cbb3 oxidases, Biochim. Biophys. Acta BBA - Bioenerg. 1655 (2004) 388–399. doi:10.1016/j.bbabio.2003.09.017.

[7] S. Ekici, G. Pawlik, E. Lohmeyer, H.-G. Koch, F. Daldal, Biogenesis of cbb3-type cytochrome c oxidase in Rhodobacter capsulatus, Biochim. Biophys. Acta. 1817 (2012) 898–910. doi:10.1016/j.bbabio.2011.10.011.

[8] C. Kulajta, J.O. Thumfart, S. Haid, F. Daldal, H.-G. Koch, Multi-step assembly pathway of the cbb3-type cytochrome c oxidase complex, J. Mol. Biol. 355 (2006) 989–1004. doi:10.1016/j.jmb.2005.11.039.

[9] G. Pawlik, C. Kulajta, I. Sachelaru, S. Schröder, B. Waidner, P. Hellwig, F. Daldal, H.-G. Koch, The Putative Assembly Factor CcoH Is Stably Associated with the cbb3-Type Cytochrome Oxidase, J. Bacteriol. 192 (2010) 6378–6389. doi:10.1128/JB.00988-10.

[10] A. Peters, C. Kulajta, G. Pawlik, F. Daldal, H.-G. Koch, Stability of the cbb3-Type Cytochrome Oxidase Requires Specific CcoQ-CcoP Interactions, J. Bacteriol. 190 (2008) 5576–5586. doi:10.1128/JB.00534-08.

[11] M.S. Muntyan, D.A. Cherepanov, A.M. Malinen, D.A. Bloch, D.Y. Sorokin, I.I. Severina, T.V. Ivashina, R. Lahti, G. Muyzer, V.P. Skulachev, Cytochrome cbb3 of

Thioalkalivibrio is a Na+-pumping cytochrome oxidase, Proc. Natl. Acad. Sci. U. S. A. 112 (2015) 7695–7700. doi:10.1073/pnas.1417071112.

[12] C.A. Carvalheda, A.V. Pisliakov, Insights into proton translocation in cbb3 oxidase from MD simulations, Biochim. Biophys. Acta BBA - Bioenerg. 1858 (2017) 396–406. doi:10.1016/j.bbabio.2017.02.013.

[13] V. Sharma, M. Wikström, V.R.I. Kaila, Dynamic water networks in cytochrome cbb3 oxidase, Biochim. Biophys. Acta BBA - Bioenerg. 1817 (2012) 726–734. doi:10.1016/j.bbabio.2011.09.010.

[14] M. Kohlstaedt, S. Buschmann, H. Xie, A. Resemann, E. Warkentin, J.D. Langer, H. Michel, Identification and Characterization of the Novel Subunit CcoM in the cbb3-Cytochrome c Oxidase from Pseudomonas stutzeri ZoBell, MBio. 7 (2016) e01921-15. doi:10.1128/mBio.01921-15.

[15] M. Kohlstaedt, S. Buschmann, J.D. Langer, H. Xie, H. Michel, Subunit CcoQ is involved in the assembly of the Cbb3-type cytochrome c oxidases from Pseudomonas stutzeri ZoBell but not required for their activity, Biochim. Biophys. Acta BBA - Bioenerg. 1858 (2017) 231–238. doi:10.1016/j.bbabio.2016.12.006.

[16] H.J.C. Berendsen, D. van der Spoel, R. van Drunen, GROMACS: A message-passing parallel molecular dynamics implementation, Comput. Phys. Commun. 91 (1995) 43–56. doi:10.1016/0010-4655(95)00042-E.

[17] S. Pronk, S. Páll, R. Schulz, P. Larsson, P. Bjelkmar, R. Apostolov, M.R. Shirts, J.C. Smith, P.M. Kasson, D. van der Spoel, B. Hess, E. Lindahl, GROMACS 4.5: a high-throughput and highly parallel open source molecular simulation toolkit, Bioinforma. Oxf. Engl. 29 (2013) 845–854. doi:10.1093/bioinformatics/btt055.

[18] J.B. Klauda, R.M. Venable, J.A. Freites, J.W. O'Connor, D.J. Tobias, C. Mondragon-Ramirez, I. Vorobyov, A.D. MacKerell, R.W. Pastor, Update of the CHARMM All-Atom Additive Force Field for Lipids: Validation on Six Lipid Types, J. Phys. Chem. B. 114 (2010) 7830–7843. doi:10.1021/jp101759q.

[19] P. Bjelkmar, P. Larsson, M.A. Cuendet, B. Hess, E. Lindahl, Implementation of the CHARMM Force Field in GROMACS: Analysis of Protein Stability Effects from Correction Maps, Virtual Interaction Sites, and Water Models, J. Chem. Theory Comput. 6 (2010) 459–466. doi:10.1021/ct900549r.

[20] R.B. Best, X. Zhu, J. Shim, P.E.M. Lopes, J. Mittal, M. Feig, A.D. Mackerell, Optimization of the additive CHARMM all-atom protein force field targeting improved sampling of the backbone φ, ψ and side-chain χ(1) and χ(2) dihedral angles, J. Chem. Theory Comput. 8 (2012) 3257–3273. doi:10.1021/ct300400x.

[21] Y.O. Ahn, P. Mahinthichaichan, H.J. Lee, H. Ouyang, D. Kaluka, S.-R. Yeh, D. Arjona, D.L. Rousseau, E. Tajkhorshid, P. Adelroth, R.B. Gennis, Conformational coupling between the active site and residues within the K(C)-channel of the Vibrio cholerae cbb3-type (C-family) oxygen reductase, Proc. Natl. Acad. Sci. U. S. A. 111 (2014) E4419-4428. doi:10.1073/pnas.1411676111.

[22] J. Hemp, H. Han, J.H. Roh, S. Kaplan, T.J. Martinez, R.B. Gennis, Comparative Genomics and Site-Directed Mutagenesis Support the Existence of Only One Input Channel for Protons in the C-Family (cbb3 Oxidase) of Heme−Copper Oxygen Reductases†, Biochemistry (Mosc.). 46 (2007) 9963–9972. doi:10.1021/bi700659y.

[23] H.J. Lee, R.B. Gennis, P. Ädelroth, Entrance of the proton pathway in cbb3-type heme-copper oxidases, Proc. Natl. Acad. Sci. 108 (2011) 17661–17666. doi:10.1073/pnas.1107543108.

[24] A.M. Waterhouse, J.B. Procter, D.M.A. Martin, M. Clamp, G.J. Barton, Jalview Version 2—a multiple sequence alignment editor and analysis workbench, Bioinformatics. 25 (2009) 1189–1191. doi:10.1093/bioinformatics/btp033.

Figure Legends

Figure 1. Overall architecture and main functional elements of *cbb*$_3$ oxidase. **(A)** A four-subunit CcoNOPM complex embedded in a membrane. Subunits N (blue), O (red), P (grey) and M (orange) are shown as cartoons. **(B)** Location and details of the BNC and the K_C-channel. Heme groups and relevant residues are shown as sticks. Cu_B and the calcium ion bridging the catalytic hemes are shown as spheres, and the bulk water is shown as a transparent surface. **(C)** "Ladder-like" interactions between subunits N (blue) and M (orange), with distances between pairs of residues shown (in Å).

Figure 2. Stability of subunit M in MD simulations. **(A)** Rmsd of the C_α atoms of the TM segment. **(B)** Rmsf of C_α atoms. **(C)** The interface between subunits N and M. The initial positions (0 ns) of both subunits are shown as transparent blue and opaque orange cartoons, respectively. Position of subunit M is also shown at the end (350 ns) of MD simulations R1 (magenta), R2 (cyan), and R3 (green). The residues involved in the "ladder-like" interactions are shown as sticks and coloured accordingly. **(D)** Predicted topology of CcoM with a transmembrane region comprising residues V7 to W29. The intensity of the blue colouring represents the degree of residue conservation based on a multiple sequence alignment of subunit CcoM from *P. stutzeri* and CcoQ subunits from γ-proteobacteria. These results were adapted from [14]: the topology was predicted using the TMHMM Server v. 2.0 (http://www.cbs.dtu.dk/services/TMHMM/), and the sequence alignment was performed with Jalview [24].

Figure 3. Internal water channels in the presence of CcoM. **(A)** Number of water molecules within 3 Å of residues in the top (H207, T215, Y251, S283, Y317, S320, T321, H345), bottom (Y223, S236, Y237, S240, H243, N289, T293), bottleneck (Y223, H243, N289,

Y317) and bifurcation (S320, T321, H345) regions of the K_C-channel. **(B)** Water occupancy in the transmembrane region is represented as a red surface (calculated within 4 Å of the residues, occupancy ≥ 10%). CcoN and CcoM are shown as blue and orange cartoons, respectively. Residues involved in the "ladder-like" interactions are shown as sticks and transparent surfaces, and residues in the K_C-channel are shown as sticks. **(C)** Number of water molecules within 3 Å of E323.

Figure 4. K_C-channel entrance region from cytoplasm. **(A)** Water occupancy within 4 Å of polar residues in the entrance region (Y223, Y235, S236, Y237, S240, H243, N289, T293, $E8^O$, $E48^P$, $E49^P$ and $N52^P$) is represented as a red mesh (occupancy ≥ 10%). The main plausible proton uptake pathways are indicated by blue arrows, and an alternative pathway in simulation R2 is shown by a dashed line. Subunit CcoP is shown in olive, and subunits CcoN, CcoP and CcoM are shown as transparent cartoons. The bulk water is shown in light blue and relevant residues are shown as sticks. **(B)** An additional water intake pathway connecting directly to the bottleneck region (via R232 and Y235) is formed in simulation R1. Representative snapshots are shown at 0, 200, 250 and 300 ns. Waters are shown as cyan sticks and as transparent blue surfaces.

Figures

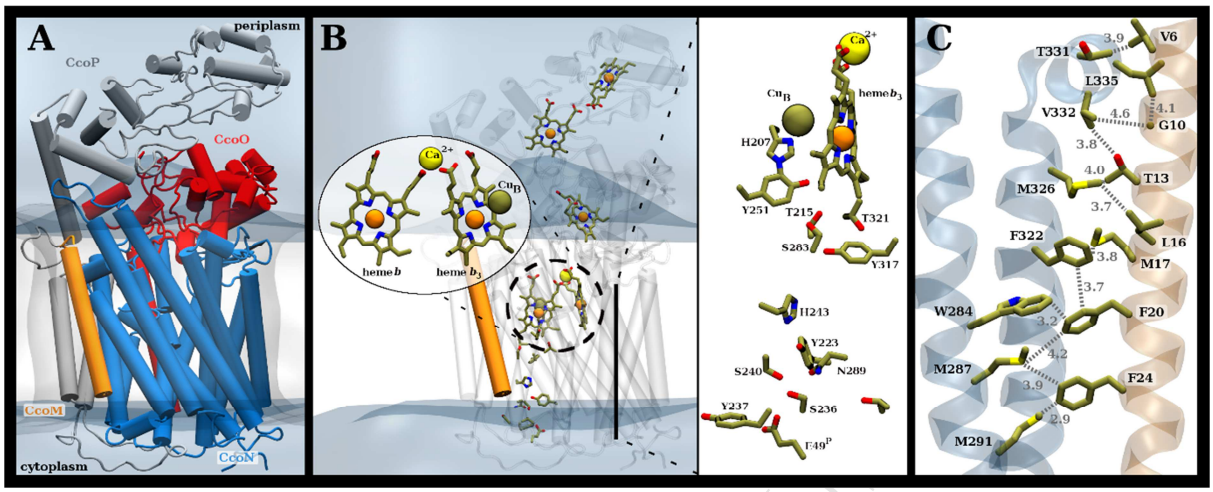

Fig. 1

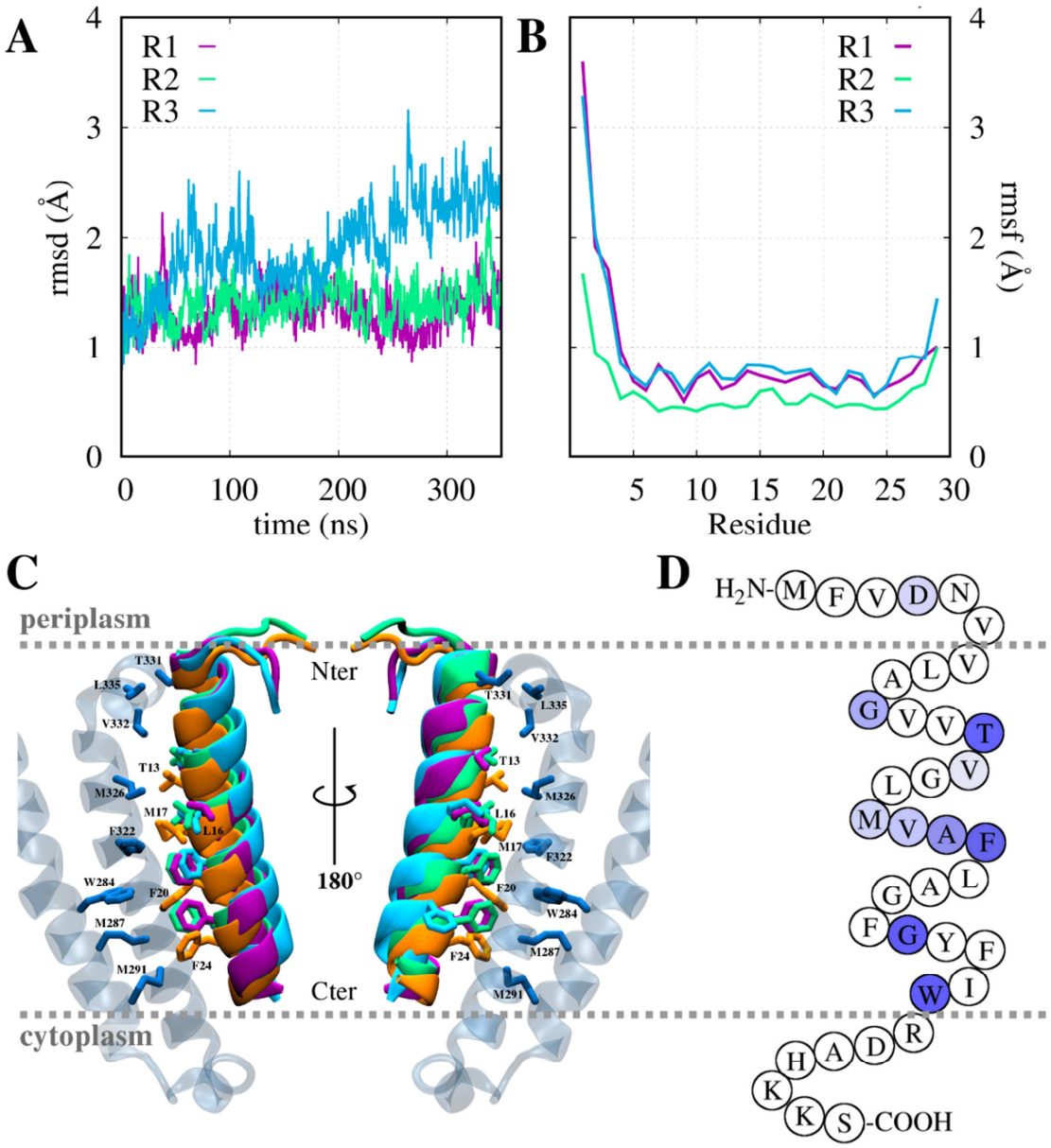
A
rmsd (Å)
time (ns)
R1
R2
R3
B
rmsf (Å)
Residue
C
periplasm
cytoplasm
Nter
Cter
180°
T331
L335
V332
T13
M326
M17
L16
F322
W284
F20
M287
F24
M291
D
H2N-MFVDNVALVGVVTLGVMVAFGALFGYFWIRHADKKS-COOH

Fig. 2

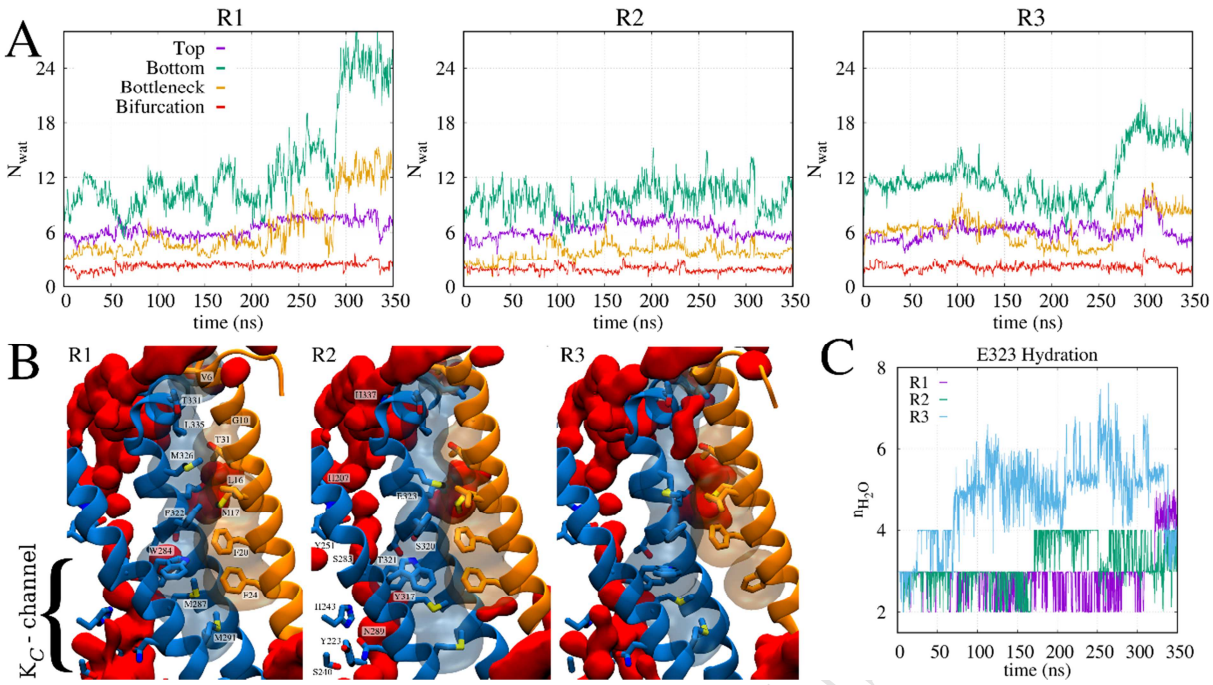

Fig. 3

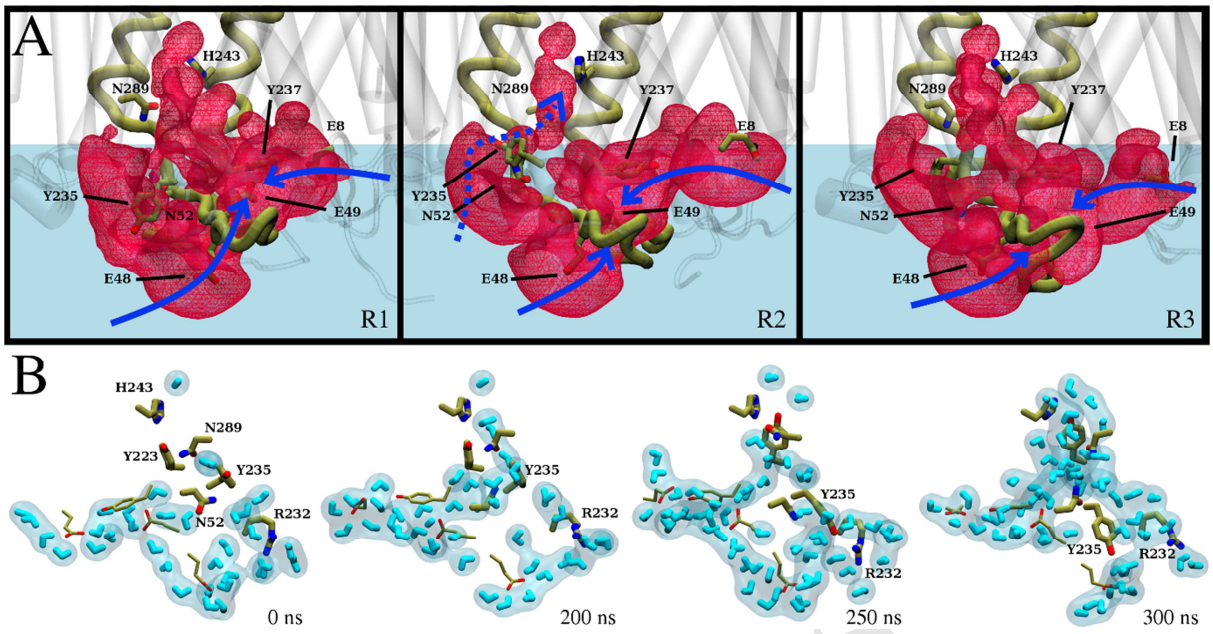

Fig. 4

Tables

Table 1. Interactions at the interface between subunits N and M.

Interactions		**Crystal structure (PDB ID: 5DJQ)**				**MD simulations**		
Sub. N	**Sub. M**	Mol.1	Mol.2	Mol.3	Mol.4	R1	R2	R3
V6	T331	3.9	4.0	4.1	4.2	3.6	3.5	3.7
G10	L335	4.1	4.2	4.0	4.0	4.2	4.1	4.5
G10	V332	4.6	4.7	4.7	5.0	4.6	4.9	5.1
T13	V332	3.8	3.9	3.8	4.1	3.8	3.8	4.3
L13	M326	4.0	3.7	4.2	3.8	3.8	3.9	4.0
L16	M326	3.7	3.7	3.8	4.3	4.9	4.8	5.3
M17	F322	3.8	4.1	3.7	3.8	3.9	3.9	4.1
F20	F322	3.7	4.2	3.7	4.1	3.9	4.0	4.8
F20	W284	3.2	3.8	3.4	3.8	6.7	4.4	6.1
F20	M287	4.2	4.5	4.8	5.0	7.1	6.8	7.2
F24	M287	3.9	4.1	4.4	4.9	4.2	4.0	8.0
F24	M291	2.9	3.5	3.0	4.5	4.6	4.8	6.2

The minimum distance between each pair of residues is shown (in Å). Mol. 1-4 refer to four different copies of the protein in the PDB file (ID: 5DJQ). MD values represent the average distances collected from the equilibrated segment (>25ns) of simulations R1-3. The standard deviation of the values obtained from MD was always lower than 1.8 Å.

Highlights

- All-atom molecular dynamics simulations of a four-subunit *cbb*$_3$ oxidase complex
- Accessory subunit CcoM is tightly bound to the core subunits through hydrophobic interactions
- CcoM does not affect internal water/proton pathways
- An additional proton channel in the putative CcoNOPH complex is not confirmed
- Functional redundancy CcoM and CcoQ is unlikely